Reprinted from Nature, Vol. 312, No. 5993, pp. 434-435, 29 November 1984

Comparative utility of microwave and shortwave satellite data for all-weather charting of snow cover

David Robinson*, Klaus Kunzi†, George Kukla* & Helmut Rott‡

* Lamont-Doherty Geological Observatory of Columbia University, Palisades, New York 10964, USA
† Institut fur Angewandte Physik, Universitat Bern, 3012 Bern, Sidlerstrasse 5, Switzerland
‡ Institut fur Meteorologie und Geophysik, Universitat Innsbruck, Schopfstrasse 41, A-6020 Innsbruck, Austria

Charting snow cover by shortwave imaging requires visual analysis which is complicated by cloud coverage and poor surface illumination[1,2]. Microwaves, however, being almost unaffected by clouds and independent of solar illumination, are potentially useful for monitoring the extent and variation in snow cover, in climatological and hydrological studies. Data from spaceborne passive microwave sensors have previously been used to chart regional overland snow cover[3-5]; but charting hemispherical snow coverage was not feasible until high spatial resolution and multiple channels were combined in the Scanning Multichannel Microwave Radiometer (SMMR) launched in 1978 on the Nimbus-7 satellite. Here we compare SMMR data with shortwave images obtained over Asia to justify further use of microwave sensors in automated charting of seasonal snow cover under all weather conditions. Agreement between the two methods is found in ~75% of the tested grid points.

Microwave radiation emitted from the Earth's surface is detected by the Scanning Multichannel Microwave Radiometer at five frequencies, in two polarization planes. Radiance in the microwave region is usually expressed by the apparent brightness temperature $T_b = eT$, where T is the physical temperature of the emitting layer and e is its emissivity ($e \leq 1$). The emission comes from throughout the snow pack as well as from the underlying ground. The discrimination of surface types is possible mainly because of differences in emissivity. Figure 1 shows some examples. Whereas a snow-free soil shows little variation in emissivity over the whole frequency range, the emissivity of dry snow decreases with increasing frequency. This decrease depends on the thickness of the scattering layer and gives an indication of the water equivalent of the dry snow. The microwave penetration depth of wet snow is small owing to the high dielectric losses of water, so that the microwave signatures of dry and wet snow differ significantly. Regions undergoing a daily freeze-thaw cycle, commonly observed over melting snow fields in spring, can be recognized by comparing day and night microwave signals. However, a snow layer which is continually wet cannot be distinguished from snow-free ground by our algorithm, which may underestimate the snow fields undergoing heavy melt[6].

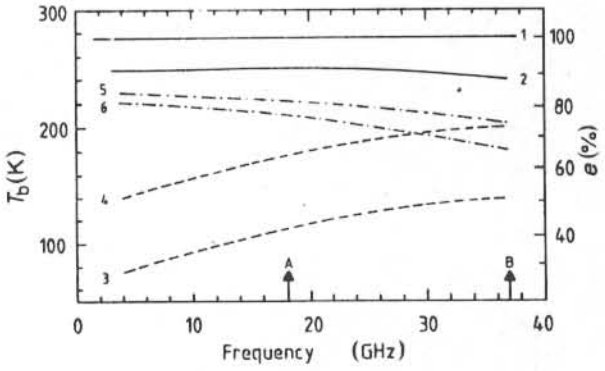

Fig. 1 Brightness temperatures (T_b) and emissivity (e) at microwave frequencies for: (1) an ideal black-body (assumed physical temperature of 273 K); (2) snow-free ground; (3) and (4) a flat sea surface, (3) horizontal and (4) vertical (physical temperature ~10 °C, incident angle ~50°); (5) snow-covered ground or old sea ice and (6) with increasing snow depth (horizontal). Curves (2), (5) and (6) are typical values obtained from ground-based microwave sensors[15] and curves (3) and (4) are based on theoretical calculations and measurements[16]. A and B mark the SMMR frequencies used for snow retrieval.

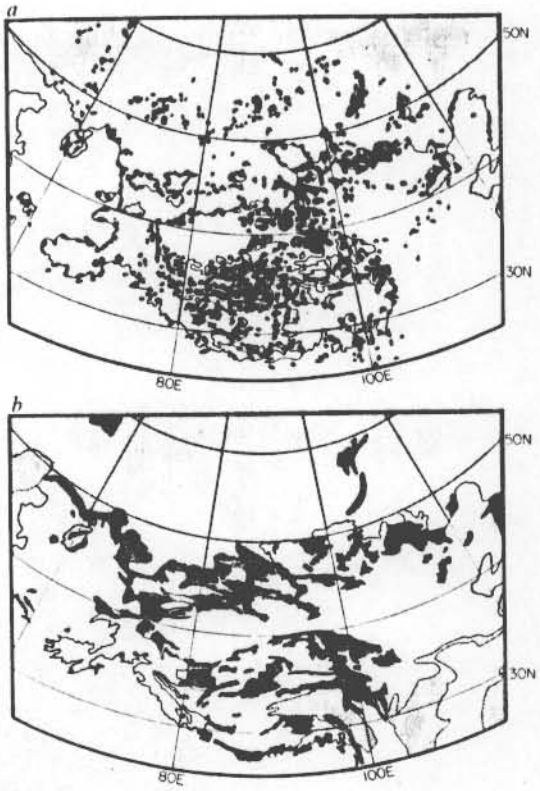

Fig. 2 Scanning Multichannel Microwave Radiometer (*a*) and Defense Meteorological Satellite Program (*b*) derived Asian snow cover for 11-15 March 1979. Fully snow-covered ground is shown in light stipple, partially covered is in dark stipple and snow-free is blank. Persistent cloudiness in *b* is hatched.

The preceding snow cover parameters can best be obtained by an analysis of the 18 and 37 GHz horizontally polarized SMMR channels[7], with spatial resolution of 60×60 km and 30×30 km, respectively. The data from three days and nights, during a five-day interval, give complete coverage for areas polewards of 25° latitude. Because of satellite power limitations, data are recorded only on alternate days. The fully automated analysis consists of reading the data from tape, applying the retrieval algorithm and displaying the data on a colour screen. A pixel is classified as covered with dry snow when the difference in brightness temperature between the 18 and 37 GHz data is less than a prescribed threshold determined empirically from tests with ground data from throughout the middle and high latitudes of the Northern Hemisphere. Additional thresholds enable further differentiation between cover of more than 10 cm and thin or patchy snow. The result shows the maximum extent of snow cover over the five day period. The algorithm is described in more detail by Kunzi *et al.*[7].

To assess the accuracy of the microwave analysis, we com-

Table 1 Comparison of microwave and shortwave-based snow classification in per cent of the total number of gridpoints

11–15 March 1979

Shortwave classification	Microwave classification: Fully snow-covered	Partially covered	Snow-free	Sum shortwave
Fully snow-covered	39.7	2.5	0.5	42.7%
Partially covered	8.4	3.5	2.6	14.5%
Snow-free	3.4	6.2	33.2	42.8%
Sum microwave	51.5%	12.2%	36.3%	

21–25 March 1979

Shortwave classification	Microwave classification: Fully snow-covered	Partially covered	Snow-free	Sum shortwave
Fully snow-covered	35.3	2.8	2.4	40.5%
Partially covered	4.5	2.7	3.1	10.4%
Snow free	6.2	7.4	35.5	49.1%
Sum microwave	46.0%	12.9%	41.0%	

pared the SMMR data with snow charts based on shortwave imagery from March 1979. The central Asian region was selected because its terrain and vegetation are highly variable, because high-quality cloud-free imagery in the visible is common at this time of the year and because it is climatologically important[8–10]. As only a limited number of ground stations in this region report snow, only remote techniques can be used.

Snow was charted from the shortwave imagery collected daily by a polar-orbiting Defense Meteorological Satellite Program sensor with a spectral range of 0.4–1.1 μm and subtrack resolution of 2.8 km (ref. 11). Imagery was available on ungridded positive film transparencies on a scale of 1 : 15 million. A trained observer examined visually the transparencies from consecutive days and plotted the snow coverage on a gridded base-chart. Snow cover was differentiated from clouds and snow-free land by its characteristic surface brightness, textures and persistence[12,13]. Two classes, full and partial cover, were distinguished. Areas where persistent clouds completely obscured the surface throughout the study period were charted as such and excluded from the analysis.

Microwave and shortwave charts for the intervals 11–15 March and 21–25 March 1979 were compared. No adjustments were made to improve the apparent agreement. Figure 2 shows the charts for 11–15 March. Grid points at the intersections of every 2.5° of longitude (50°E–140°E) and 1° of latitude (28°N–60°N) were categorized according to charted microwave and shortwave conditions. The results are shown in Table 1. Only 3.5% and 4.5% of the 924 gridpoints analysed on the 11–15 March and 21–25 March charts, respectively, were excluded because of persistent cloud cover. However, in other seasons clouds are more frequent in this region. Areas classified on the microwave charts as having dry snow deeper than 10 cm were assumed to be fully covered.

There is reasonable agreement between the microwave and shortwave classifications of surface conditions. Complete agreement is found over 76.4% (11–15 March) and 73.5% (21–25 March) of the area, whereas only 3.9% and 8.6% show full snow cover in one chart and no snow in the other (Table 1).

The best agreement between the charts occurs in areas where shortwave charts show full cover and where microwave charts show snow-free ground. Microwave charts tend to indicate more snow than the visual analysis. This is true for situations where partially covered areas in microwave analyses are classified as snow free in shortwave charts, and where full cover on microwave charts is seen as partial cover in the shortwave. Disagreement is most frequently observed over the Tibetan plateau, where snow-free ground intersperses the snow-capped mountains. Possible reasons for this are: (1) the much higher spatial resolution of the shortwave chart enables the recognition of individual snow patches covering only a small portion of an area, whereas microwave signals from these snow patches are combined with those of the adjacent snow-free ground and the area as a whole is classified as partially snow-covered; (2) imagery employed in this study may reflect time differences of up to 4 days, so that the snow observed in one set may have been absent in the other; (3) night-time dry-sand microwave signatures are similar to those of thin dry-snow layers because the frequency-dependent penetration depth in dry sand is approximately several wavelengths and vertical temperature gradients in the sand on clear nights are strong.

The Scanning Multichannel Microwave Radiometer has now provided satellite data for almost six consecutive winter seasons in the Northern Hemisphere. Additional tests with shortwave satellite images and, where available, correlative ground data will further our understanding of the microwave data set. At present the multispectral microwave method appears to be very promising for automated large-scale charting of snow. This will prove invaluable, especially in autumn and early winter when snow fields develop in poorly illuminated areas under heavy cloud cover, making conventional charting difficult and inaccurate[14]. However, full substitution of shortwave snow-cover analysis by microwave mapping will not be possible in climate studies as one of the most critical snow parameters, its high albedo, cannot be assessed using microwaves.

We thank Michael Fried for assistance with the shortwave analysis. This project was supported by the Swiss National Science Foundation, the Austrian Funds zur Forderung der Wissenschaftlichen Forschung and NSF contract ATM82-00863. This is Lamont-Doherty Geological Observatory contribution no. 3730.

Received 4 June; accepted 18 September 1984.

1. Smigielski, F. *Glaciological Data* **11**, 63–69 (1981).
2. Matson, M. & Wiesnet, D. *Nature* **289**, 451–456 (1981).
3. Kunzi, K. & Staelin, D. *Proc. Tenth Int. Symp. Remote Sensing Envir.*, Ann Arbor, 1245–1253 (1975).
4. Fisher, A., Ledsham, B., Rosenkranz, P. & Staelin, D. *Proc. Symp. Met. Obsns from Space: Their Contr. to First GARP Global Exp.* 98–103 (Cospar 1976).
5. Foster, J. *et al. Remote Sensing Envir.* **10**, 285–298 (1980).
6. Patil, S., Kunzi, K. & Rott, H. *11th Eur. Microwave Conf.*, Amsterdam, 227–232 (1981).
7. Kunzi, K., Patil, S. & Rott, H. *IEEE Trans. Geosci. Remote Sensing* **20**, 452–467 (1982).
8. Hahn, D. & Shukla, J. *J. atmos. Sci.* **33**, 2461–2462 (1976).
9. Gao, Y., Tang, M., Luo, S., Shen, Z. & Li, C. *Bull. Am. met. Soc.* **62**, 31–35 (1981).
10. Dey, B. & Bhandu Kumar, O. S. R. U. *J. appl. Met.* **21**, 1929–1932 (1982).
11. Fett, R. & Bohan, W. *NAVENVPRECRSCHFAC Applic. Rep. 77-03*, 1, (1977).
12. Kukla, G., Robinson, D. & Brown, J. *Glaciological Data* **11**, 87–91 (1981).
13. Robinson, D. thesis, Columbia Univ. (1984).
14. Kukla, G. & Robinson, D. *Glaciological Data* **11**, 103–119 (1981).
15. Maetzler, C., Schanda, E. & Good, W. *IEEE Trans. Geosci. Remote Sensing* **20**, 57–66 (1982).
16. NORSEX Group, *Science* **220**, 781–787 (1983).

Printed in Great Britain by Macmillan Production Ltd., Basingstoke, Hampshire